Applied Catalysis B: Environmental 180 (2016) 766–774

Contents lists available at ScienceDirect

Applied Catalysis B: Environmental

journal homepage: www.elsevier.com/locate/apcatb

Promotional effect of Nb additive on the activity and hydrothermal stability for the selective catalytic reduction of NO_x with NH_3 over $CeZrO_x$ catalyst

Shipeng Ding, Fudong Liu*, Xiaoyan Shi, Hong He**

State Key Joint Laboratory of Environment Simulation and Pollution Control, Research Center for Eco-Environmental Sciences, Chinese Academy of Sciences, 18 Shuangqing Road, Haidian District, Beijing 100085, PR China

ARTICLE INFO

Article history:
Received 23 April 2015
Received in revised form 21 June 2015
Accepted 26 June 2015
Available online 17 July 2015

Keywords:
Selective catalytic reduction
Nitrogen oxides
Diesel engine exhaust
Hydrothermal stability
$CeNbZrO_x$ mixed oxide

ABSTRACT

The promotional mechanism of Nb addition on the activity and hydrothermal stability of $CeZr_2O_x$ catalyst for the selective catalytic reduction of NO_x with NH_3 (NH_3-SCR) was investigated by various methods including N_2-physisorption, XRD, H_2-TPR and *in situ* DRIFTS. The Nb-promoted $CeZr_2O_x$ catalyst showed remarkable NH_3-SCR activity together with excellent N_2 selectivity, SO_2/H_2O resistance and outstanding hydrothermal stability. The characterization results showed that the introduction of Nb to $CeZr_2O_x$ not only resulted in the high surface area and strong redox ability, but also promoted the adsorption and activation of NH_3 and enhanced the reactivity of adsorbed nitrate together with NH_3 species. All the above features were favorable for the superior NH_3-SCR performance. In addition, the $CeNb_{3.0}Zr_2O_x$ catalysts hydrothermally aged below 800 °C still possessed high redox ability and abundant acid sites, all of which were responsible for the excellent hydrothermal durability. The novel $CeNb_{3.0}Zr_2O_x$ catalyst was a promising candidate for the removal of NO_x from diesel engine.

1. Introduction

Nitrogen oxides (NO_x), emitted from mobile resources such as diesel engines and stationary resources like coal-fired power plants have been major atmospheric pollutants. The selective catalytic reduction of NO_x with NH_3 (NH_3-SCR) is the most widely employed technique to control the emission of NO_x, and the most commercially used catalyst is V_2O_5–WO_3/TiO_2 [1–3]. However, there still remains room for improvement with this catalyst system, such as low hydrothermal stability, a narrow operating temperature window and the unselective oxidation of NH_3 which produces ozone-depleting N_2O at high temperatures [2,4,5]. Consequently, it is of great significance to develop novel NH_3-SCR catalysts, with outstanding low-temperature NO_x conversion, high N_2 selectivity, excellent hydrothermal stability and a broad operating temperature window, which will substitute for the conventional V_2O_5–WO_3/TiO_2 catalyst.

CeO_2 was used as oxygen storage component of conventional three-way catalysts (TWCs) in the late 1980s [6]. However, pure CeO_2 showed poor stability and was susceptible sintering at high temperatures. The introduction of ZrO_2 to CeO_2 resulted in effectively improving the thermal stability of CeO_2 [6,7]. In model Pd three-way catalysts, catalysts prepared on the $CeZrO_x$ solid solution retained larger oxygen storage capacity than those based on pure CeO_2 after aging [7]. The $CeZrO_x$ is considered to be one of the most promising materials for NO_x removal [8]. It was reported that the WO_3/CeO_2–ZrO_2 catalyst exhibited nearly 100% NO_x conversion in the temperature range of 200–500 °C, and also showed higher thermal stability in comparison to the conventional V_2O_5–WO_3/TiO_2 catalyst in NH_3-SCR reaction [9]. Gao et al. developed a novel Ce catalyst supported on sulfated ZrO_2 for NH_3-SCR reaction, which showed superior catalytic activity due to the well dispersion of CeO_2, abundant acid sites together with increasing surface area and enrichment of Ce^{3+} after sulfation [10]. $Ce_{0.75}Zr_{0.25}O_2$–PO_4^{3-} catalyst prepared by impregnating phosphates on $Ce_{0.75}Zr_{0.25}O_2$ still presented high SCR activity at 300–400 °C after hydrothermal-aged at 760 °C for 48 h, which might result from the fact that phosphates improved NH_3 adsorption and suppressed the unselective oxidation of NH_3 at high temperatures [11]. It was also found that the morphology of $CeZrO_x$ had a significant influence on the performance of MnO_x/CeO_2–ZrO_2 catalyst for the NH_3-SCR

* Corresponding author. Present address: Materials Sciences Division, Lawrence Berkeley National Laboratory, 1 Cyclotron Road, Berkeley, CA 94720, United States.
** Corresponding author. Fax: +86 10 62849123.
E-mail addresses: fudongliu@lbl.gov, lfd1982@gmail.com (F. Liu), honghe@rcees.ac.cn (H. He).

http://dx.doi.org/10.1016/j.apcatb.2015.06.055
0926-3373/

reaction, and MnO_x/CeO_2–ZrO_2 nanorods exhibited higher activity than nanotubes and nanopolyhedra [12]. $MnO_x/Ce_{0.9}Zr_{0.1}O_2$ nanorods exhibited better NO_x reduction activity than $Ce_{0.9}Zr_{0.1}O_2$. At the same time, experimental results together with density functional theory calculations clearly demonstrated that MnO_x species could easily form an oxygen vacancy distortion and were highly dispersed on the surface of $Ce_{0.9}Zr_{0.1}O_2$ nanorods [13].

In addition, Nb-containing compounds and materials are currently essential catalysts for a variety of reactions, like the hydrogenation of alkane and the catalytic removal of nitrogen oxides [14]. It was reported that the NH_3-SCR reactivity of Nb-containing MnO_x–CeO_2 was dramatically improved as a result of Nb addition, and the characterization results indicated that the strong interaction between Nb and Mn catalytic active sites resulted in a remarkable dispersion of the oxidizing sites together with acidic sites and inhibited the unselective NH_3 oxidation at high temperatures [15]. CeO_2–Nb_2O_5 catalyst containing abundant surface absorbed oxygen, which might result from the short-range activation effect of Nb to Ce species, also exhibited excellent SCR performance [16].

Therefore, in the present work, a series of Nb-promoted $CeZr_2O_x$ catalysts was prepared by a homogeneous precipitation method and was applied in the NH_3-SCR process. The obtained $CeNb_{3.0}Zr_2O_x$ catalyst exhibited excellent SCR activity, N_2 selectivity, SO_2/H_2O resistance and hydrothermal durability. The structure, redox ability and reactivity of adsorbed NO_x and NH_3 species on the catalysts were systematically characterized using various methods including N_2 physisorption, XRD, H_2-TPR and *in situ* DRIFTS. The characterization results indicated that the addition of Nb significantly improved the surface area, redox ability and reactivity of adsorbed nitrate together with NH_3 species. High redox ability and abundant acid sites still existed on $CeNb_{3.0}Zr_2O_x$ catalysts hydrothermally aged below 800 °C.

2. Experimental

2.1. Catalysts preparation and activity test

A homogeneous precipitation method using urea as precipitant was applied to prepare the pure Nb_2O_5 and $CeNb_aZr_2O_x$ catalysts. In a typical preparation process, the desired amount of $Ce(NO_3)_3{\cdot}6H_2O$, $NbCl_5$ and $Zr(NO_3)_4{\cdot}5H_2O$ were dissolved in deionized water, respectively. Superfluous urea was then added into the mix solution, with continuous stirring at 90 °C for 12 h. Subsequently, the precipitate was collected by filtration and washing with excess deionized water, dried at 100 °C overnight and calcined at 500 °C for 3 h. The catalysts were denoted as $CeNb_aZr_2O_x$ (a = 0, 0.5, 1.0, 3.0, 6.0) where a represented the molar ratio of Nb/Ce, and the Ce/Zr molar ratio was fixed at 1:2. The expected weight percentages of components in $CeNb_aZr_2O_x$ catalysts are shown in Table S1 in Supporting information. For comparison, commercial V_2O_5-WO_3/TiO_2 catalyst with 2 wt.% V_2O_5 and 10 wt.% WO_3 was also prepared using the conventional impregnation method. All the catalysts were crushed and sieved to 40–60 mesh for activity evaluation.

The hydrothermal-aged $CeNb_{3.0}Zr_2O_x$ catalysts were also obtained by treating the fresh samples in air containing 10 vol.% H_2O at desired temperature for 8 h or 48 h with a GHSV of 10,000 h^{-1}. The hydrothermal-aged samples were denoted as $CeNb_{3.0}Zr_2O_x$-t, where t represented the treatment temperature in °C.

The NH_3-SCR activity of samples was performed in a fixed-bed quartz tube reactor at atmospheric pressure. The experimental conditions were as follows: 500 ppm NO, 500 ppm NH_3, 5 vol.% O_2, 100 ppm SO_2 (when used), 5 vol.% H_2O (when used), N_2 balance and flow rate of 500 mL/min. The effluent gas was continuously analyzed by an FTIR spectrometer (Nicolet Nexus 670) which was equipped with a heated, low volume multiple-path gas cell (2 m). The FTIR spectra were collected after 1 h while the NH_3-SCR reaction reached a steady state. NO_x conversion and N_2 selectivity were calculated as follows:

$$NO_x\ \text{conversion} = \left(1 - \frac{[NO]_{out} + [NO_2]_{out}}{[NO]_{in} + [NO_2]_{in}}\right) \times 100\%$$

$$N_2\ \text{selectivity} = \frac{[NO]_{in} + [NH_3]_{in} - [NH_2]_{out} - 2[N_2O]_{out}}{[NO]_{in} + [NH_3]_{in}} \times 100\%$$

2.2. Characterization

The N_2 adsorption–desorption isotherms over Nb_2O_5, $CeNb_aZr_2O_x$ and hydrothermal-aged $CeNb_{3.0}Zr_2O_x$ catalysts were achieved using a Quantachrome Autosorb-1C instrument at liquid N_2 temperature (77 K). Before the N_2 physisorption, all the catalysts were outgassed at 300 °C for 5 h in vacuum. The specific surface areas were calculated by BET equation at P/P_0 in the partial pressure range of 0.05–0.35.

Powder X-ray diffraction (XRD) patterns of the samples were conducted on a computerized PANalytical X'Pert Pro diffractometer with Cu Kα (λ = 0.15406 nm) radiation. The data of 2θ from 20 to 80° were collected at a step of 8°/min with the step size of 0.07°.

The H_2-TPR experiments were carried out on a Micromeritics AutoChem 2920 chemisorption analyzer. In a typical measurement, 100 mg of the sample was firstly preprocessed in a flow of 20 vol.% O_2/N_2 with the total flow rate of 50 mL/min at 400 °C for 0.5 h, and then lowered the temperature to ambient temperature (30 °C) followed by Ar purging for another 0.5 h. Then the temperature was linearly increased from 30 to 1000 °C at the heating rate of 10 °C/min in a flow of 10 vol.% H_2/Ar (50 mL/min). The H_2 consumption amount was detected by a thermal conductivity detector (TCD).

The *in situ* DRIFTS experiments were performed on an FTIR spectrometer (Nicolet Nexus 670) equipped with a smart collector and an MCT/A detector, which was cooled by liquid nitrogen. Prior to each experiment, the catalyst was pretreated in 20 vol.% O_2/N_2 at 400 °C for 0.5 h and then cooled down to 200 °C. The background spectrum which was collected in flowing N_2 was automatically subtracted from the sample spectrum. The reaction conditions were as follows: 500 ppm NH_3, 500 ppm NO, 5 vol.% O_2, N_2 balance and 300 mL/min total flow rate. All spectra were recorded by accumulating 100 scans with a resolution of 4 cm^{-1}.

3. Results and discussion

3.1. NH_3-SCR activity

The NO_x conversion and N_2 selectivity in NH_3-SCR reaction over pure Nb_2O_5 and $CeNb_aZr_2O_x$ catalysts with different Nb contents under a GHSV of 50,000 h^{-1} are shown in Fig. 1. $CeZr_2O_x$ exhibited low NO_x conversion, poor N_2 selectivity along with a narrow operating temperature window, and the maximum NO_x conversion was only 90% at 350 °C. Pure Nb_2O_5 sample showed negligible SCR activity and the NO_x conversion was below 10% in the whole temperature range. Nevertheless, for Nb-containing $CeNb_aZr_2O_x$ catalysts, the addition of Nb resulted in a great enhancement of NO_x conversion both in low and high temperatures, high N_2 selectivity and a broad temperature window, which indicated that the coexistence of Nb and $CeZr_2O_x$ species was of essential importance for high NH_3-SCR performance. $CeNb_{3.0}Zr_2O_x$ catalyst with the molar ratio of Nb:Ce = 3.0:1 showed the highest NH_3-SCR performance in the entire temperature range, over which the complete removal of NO_x was accomplished from 225 to 425 °C under the GHSV of 50,000 h^{-1}. The NO_x conversion was over 90% above 250 °C

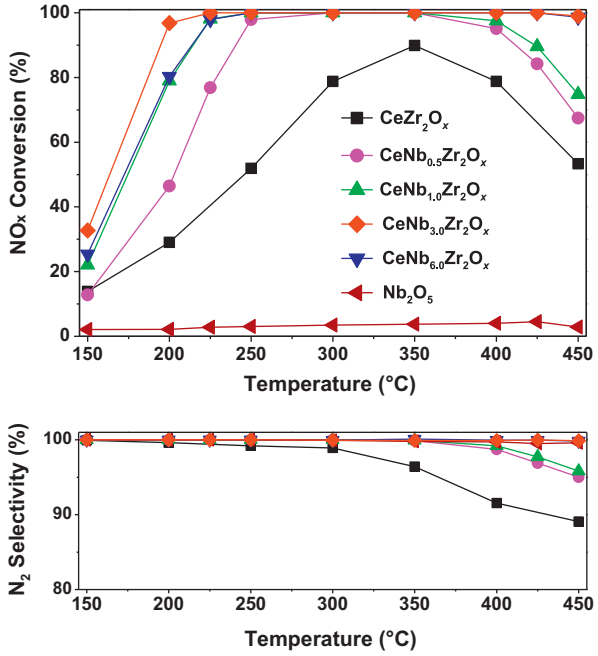

Fig. 1. NO_x conversion and N_2 selectivity as a function of temperature over pure Nb_2O_5 and $CeNb_aZr_2O_x$ (a = 0, 0.5, 1.0, 3.0, 6.0) catalysts in NH_3-SCR reaction. Reaction conditions: [NO] = [NH_3] = 500 ppm, [O_2] = 5 vol.%, GHSV = 50,000 h^{-1}.

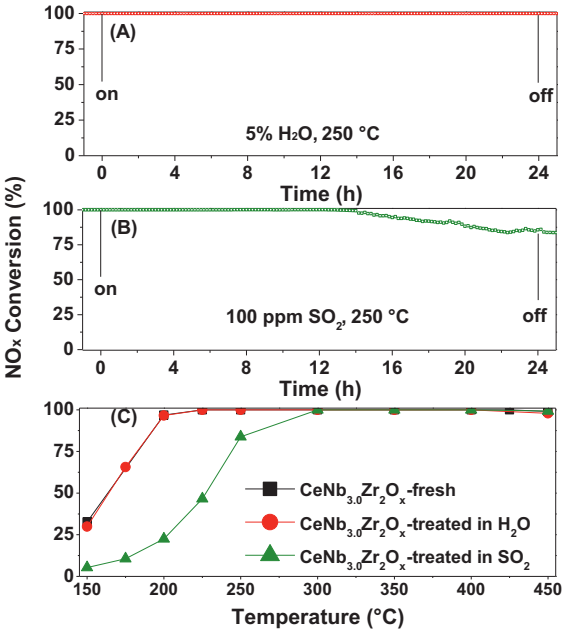

Fig. 2. The effect of H_2O (A), SO_2 (B) on NH_3- SCR activity over $CeNb_{3.0}Zr_2O_x$ catalyst with 5 vol.% H_2O or 100 ppm SO_2 at 250 °C; (C) NO_x conversion in NH_3-SCR reaction as a function of temperature without H_2O and SO_2 over $CeNb_{3.0}Zr_2O_x$ catalysts after treatment in H_2O/SO_2 for 24 h. Reaction conditions: [NO] = [NH_3] = 500 ppm, [O_2] = 5 vol.%, [SO_2] = 100 ppm (when used), [H_2O] = 5 vol.% (when used), GHSV = 50,000 h^{-1}.

even under a quite high GHSV of 200,000 h^{-1} (see Fig. S1), which indicated that the obtained catalyst exhibited excellent resistance to high space velocity and was suitable to applications of diesel engines where there was only limited space for the installation of SCR catalysts. For conventional V_2O_5–WO_3/TiO_2 catalyst, one of the inevitable drawbacks was the unselective oxidation of NH_3 at high temperatures, which would lower the NO_x conversion and produce a large amount of N_2O. However, the N_2 selectivity of novel $CeNb_{3.0}Zr_2O_x$ catalyst was as high as over 99% even at 450 °C, which was promising for the elimination of NO_x from diesel engine exhaust. Further increasing the molar ratio of Nb/Ce from 3.0:1 to 6.0:1 would lead to a slight decrease of NO_x conversion at low temperature, probably due to the coverage of active cerium sites by excess Nb species. In addition, the NH_3 conversion in NH_3-SCR reaction over $CeZr_2O_x$ and $CeNb_{3.0}Zr_2O_x$ is presented in Fig. S2. The results indicated that the introduction of Nb greatly improved the conversion of NH_3 at low temperatures, and the NH_3 was almost completely consumed over $CeZr_2O_x$ and $CeNb_{3.0}Zr_2O_x$ samples at high temperatures. The NH_3-SCR results indicated that some synergistic effect possibly exist between Nb, Ce and Zr species, which will be discussed later in this work.

3.2. Effect of H_2O and SO_2

In practical applications, the combustion exhaust containing water vapor and SO_2 may lead to the deactivation of NH_3-SCR catalyst. Therefore, it was worthwhile to investigate the influence of H_2O/SO_2 on the activity over $CeNb_{3.0}Zr_2O_x$ catalyst. As shown in Fig. 2(A), the addition of 5 vol.% H_2O had a negligible inhibition effect on the NH_3-SCR performance of $CeNb_{3.0}Zr_2O_x$ and the NO_x conversion was almost 100% for the entire 24 h, suggesting that $CeNb_{3.0}Zr_2O_x$ catalyst exhibited strong resistance to H_2O poisoning at 250 °C. The effect of 100 ppm SO_2 on $CeNb_{3.0}Zr_2O_x$ catalyst activity is shown in Fig. 2(B). The NO_x conversion did not show any decrease for the first 14 h when SO_2 was introduced into the reaction atmosphere. However, further increasing the reaction time resulted in a slight decline and reduced to 80%, due to the deposition of ammonium sulfate/bisulfate on the surface, which might block the active sites. In order to further study the influence of H_2O/SO_2 poisoning on the performance of the catalysts treated in the NH_3-SCR reaction at 250 °C for 24 h, the activity of $CeNb_{3.0}Zr_2O_x$ samples in Fig. 2(A) and (B) was retested in the absence of H_2O and SO_2 and the results are shown in Fig. 2(C). It was obvious that $CeNb_{3.0}Zr_2O_x$ after treatment in H_2O showed high activity, and nearly 100% NO_x conversion was obtained between 200 and 450 °C, which was almost the same as that of the fresh catalyst. Even though the SO_2 treatment had a negative effect on the activity of $CeNb_{3.0}Zr_2O_x$, the NO_x conversion was still more than 80% above 250 °C. In short summary, the $CeNb_{3.0}Zr_2O_x$ catalyst exhibited high resistance to H_2O and SO_2 poisoning, especially when the temperature was more than 250 °C, and could be used to eliminate the NO_x from diesel engine exhaust containing a handful of H_2O and SO_2.

3.3. Promotional effect of Nb addition on the SCR activity

3.3.1. N_2 physisorption

Fig. S3 shows the N_2 adsorption–desorption isotherms of the catalysts. It could be observed that all the samples displayed type IV isotherms in the relative pressure (P/P_0) range of 0.4–0.8 according to the IUPAC classification, which were typical for mesoporous materials (2–50 nm) [17]. In addition, the BET surface area and

Table 1
BET surface area and pore volume of Nb_2O_5 and $CeNb_aZr_2O_x$ samples.

Catalysts	S_{BET}[a] (m^2/g)	Pore volume[b] (cm^3/g)
Nb_2O_5	68.4	0.11
$CeZr_2O_x$	107.3	0.13
$CeNb_{0.5}Zr_2O_x$	170.1	0.25
$CeNb_{1.0}Zr_2O_x$	198.1	0.20
$CeNb_{3.0}Zr_2O_x$	208.7	0.18
$CeNb_{6.0}Zr_2O_x$	206.5	0.17

[a] BET surface area.
[b] Total pore volume.

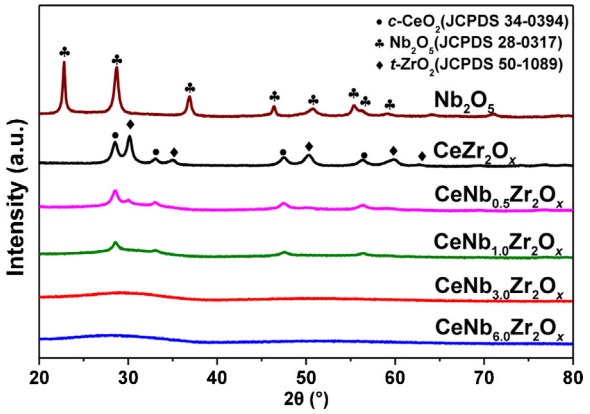

Fig. 3. Powder XRD of Nb_2O_5 and $CeNb_aZr_2O_x$ catalysts with different Nb loadings.

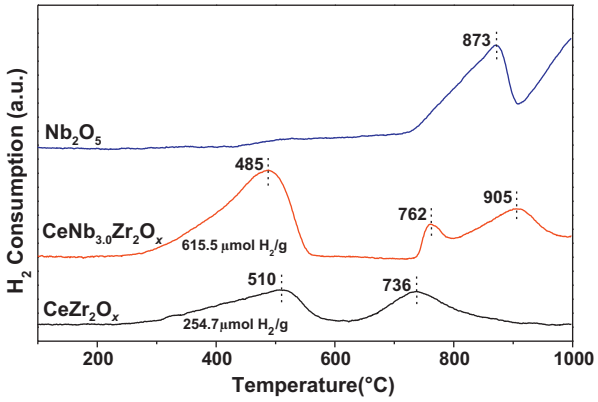

Fig. 4. H_2-TPR profiles of Nb_2O_5, $CeZr_2O_x$ and $CeNb_{3.0}Zr_2O_x$ catalysts.

pore volume derived from N_2 physisorption results of Nb_2O_5 and $CeNb_aZr_2O_x$ samples are shown in Table 1. It was obvious that the addition of Nb_2O_5 to $CeZr_2O_x$ had a great influence on the surface and pore volume of the samples. As the molar ratio of Nb/Ce increased from 0.5:1 to 3.0:1, the surface area of the corresponding samples grew significantly. $CeNb_{3.0}Zr_2O_x$ catalyst, with molar ratio of Nb/Ce = 3.0:1, showed the largest surface area of 208.7 m^2/g among the Nb-containing catalysts, which was in consistent with the best NH_3-SCR performance. However, further improving the Nb/Ce molar ratio to 6.0:1 led to a slight decrease of the surface area. It was believed that, compared to $CeNb_{3.0}Zr_2O_x$ catalyst, $CeNb_{6.0}Zr_2O_x$ catalyst showed a slight decrease of NO_x conversion at low temperature, which possibly result from the coverage of active cerium sites by excess Nb species rather than the decline of surface area. These results indicated that the introduction of Nb could induce structural modification of the samples and lead to a higher surface area, which was beneficial for the dispersion of active components and resulted in high NO_x conversion over Nb-containing catalysts for NH_3-SCR [18].

3.3.2. XRD results

Powder XRD was conducted to investigate the crystal structural of Nb_2O_5 and $CeNb_aZr_2O_x$ catalysts, and the results are shown in Fig. 3. The $CeZr_2O_x$ catalyst provided typical diffraction patterns for the ZrO_2 tetragonal phase (JCPDS 50-1089) and the CeO_2 cubic phase (JCPDS 34-0394), which indicated that no strong interaction existed between Ce and Zr, leading to the segregation of CeO_2 and ZrO_2 crystallites [19]. With the improvement of Nb/Ce molar ratio, the band intensity ascribed to CeO_2 and ZrO_2 over Nb-containing catalysts decreased significantly. No diffraction peaks attributed to Nb species were detected in the XRD patterns for all the Nb-containing catalysts, indicating that Nb species existed as amorphous. For $CeNb_{3.0}Zr_2O_x$ and $CeNb_{6.0}Zr_2O_x$ catalysts, no obvious peak attributed to CeO_2 or ZrO_2 was observed suggesting the formation of homogeneously dispersed crystallites or a complete amorphous structure. Amorphous structure usually possessed larger surface area than the crystallized one [20], which might be one of the essential reasons why the surface area of Nb-containing catalysts was higher than that of $CeZr_2O_x$ catalyst.

3.3.3. H_2-TPR

H_2-TPR experiments were performed to investigate the redox ability of Nb_2O_5, $CeZr_2O_x$ and $CeNb_{3.0}Zr_2O_x$ catalysts, and the results are shown in Fig. 4. For the $CeZr_2O_x$ catalyst, the reduction peak at about 510 °C was assigned to the reduction of surface Ce^{4+} to Ce^{3+}, and the peak at 736 °C could be attributed to the reduction of bulk CeO_2 [21–23]. In addition, the reduction peak of Nb_2O_5 was about 873 °C, which was responsible for reduction of bulk Nb_2O_5 to Nb_2O_4 [16,24]. Over $CeNb_{3.0}Zr_2O_x$ catalyst, three reduction peaks centered at about 485, 762 and 905 °C were observed. The two peaks at higher temperature belonged to the reduction of bulk CeO_2 and Nb_2O_5, respectively. The reduction peak at 485 °C, which was ascribed to the reduction of surface Ce^{4+} to Ce^{3+} showed lower reduction temperature in comparison to $CeZr_2O_x$ sample, which indicated that redox ability of $CeNb_{3.0}Zr_2O_x$ was greatly improved after the addition of Nb. Higher redox ability of $CeNb_{3.0}Zr_2O_x$ could enhance the mobility of surface oxygen due to the strong synergetic effect among Zr, Ce and Nb species. It was believed that the synergetic effect led to severe structural distortion and affluent oxygen defects [25,26]. The oxygen defects promoted oxygen diffusion from the subsurface layers and might progressively proceed deeper into the bulk [27,28]. Furthermore, the H_2 consumption for the reduction of surface Ce^{4+} to Ce^{3+} was calculated and the values are listed in Fig. 4. The results in Table S1 showed that the weight percentage of CeO_2 in $CeNb_{3.0}Zr_2O_x$ was lower than that in $CeZr_2O_x$. However, the H_2 consumption of $CeNb_{3.0}Zr_2O_x$ was 615.5 μmol H_2/g_{cat}, which was higher than that of $CeZr_2O_x$ (254.7 μmol H_2/g_{cat}), indicating the formation of more reducible Ce species after the introduction of Nb to $CeZr_2O_x$. All the above features were beneficial for the excellent SCR activity.

3.3.4. NH_3 and NO_x adsorption ability

The *in situ* DRIFTS of NH_3 adsorption at 200 °C was conducted to investigate the differences of acidity on the catalysts after Nb introduction and the results are illustrated in Fig. 5(A). After exposure to NH_3 and N_2 purge, the catalyst surface was mainly covered by a couple of NH_3 species. The bands centered at 1603 cm^{-1} and 1209, 1263, 1193, 1182 cm^{-1} were assigned to asymmetric and symmetric bending vibrations of the N—H bonds in coordinated NH_3 linked to Lewis acid sites, respectively [29–31]. In addition, the bands at 3360, 3260 and 3155 cm^{-1} were ascribed to N—H stretching modes of coordinated NH_3 [32]. The bands at 1668 cm^{-1} and 1434, 1444, 1414 cm^{-1} attributed to symmetric and asymmetric bending vibrations of NH_4^+ species on Brønsted acid sites were also observed [4,33–36]. Several negative bands around 3700 cm^{-1} ascribed to the hydroxyl consumption were also found, which might result from the reaction between hydroxyl and NH_3 [4,25].

Pure Nb_2O_5 showed slight amount of Brønsted acid sites and Lewis acid sites. However, the introduction of Nb to $CeZr_2O_x$ resulted in more acid sites on the catalysts. $CeNb_{3.0}Zr_2O_x$ catalyst, with Nb/Ce molar ratio of 3.0:1, exhibited the largest amount of NH_4^+ bound to Brønsted acid sites and NH_3 linked to Lewis acid sites among the series catalysts, which was quite in accordance with its highest NH_3-SCR performance. It has been reported that the surface acidity of NbO_x–MnO_x–CeO_2 was significantly increased as a result of Nb addition [37]. In addition, the Nb—OH bond was

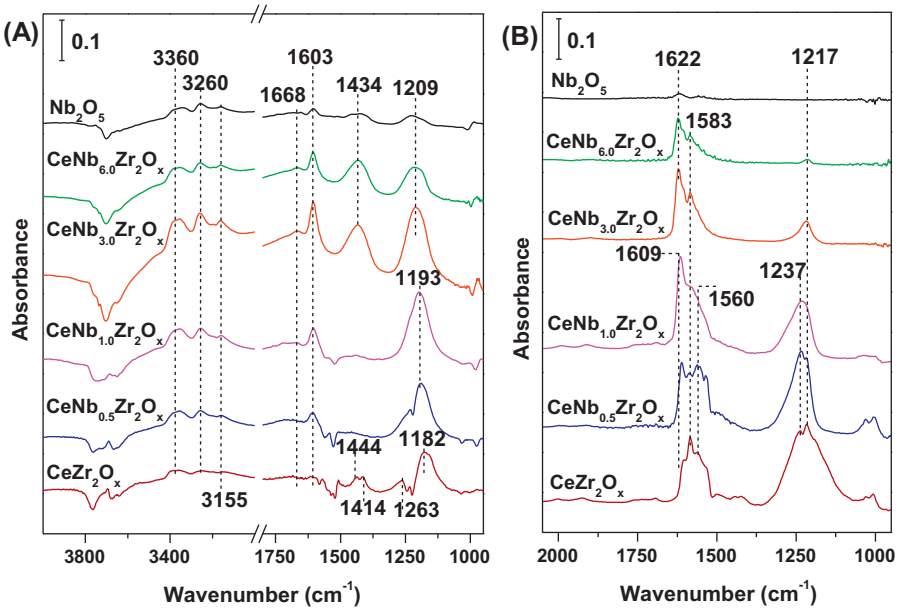

Fig. 5. *In situ* DRIFTS of 500 ppm NH_3 adsorption (A) and 500 ppm NO + 5 vol.% O_2 adsorption (B) with 300 mL/min flow rate at 200 °C on Nb_2O_5 and $CeNb_aZr_2O_x$ series catalysts.

responsible for the Brønsted acid site and Nb=O bond for the Lewis acid site [16]. Further increasing the Nb/Ce molar ratio from 3.0 to 6.0 led to a slight decrease of acid sites. In addition, the desorption of adsorbed NH_3 species at various temperatures over $CeZr_2O_x$ and $CeNb_{0.3}Zr_2O_x$ catalysts showed that $CeZr_2O_x$ showed negligible amount of NH_3 species at 350 °C, while several bands still remained on $CeNb_{3.0}Zr_2O_x$ sample (see Fig. S4). The results indicated that the introduction of Nb enhanced both the amount and strength of acid sites, which were beneficial for the adsorption together with activation of NH_3, leading to an excellent NH_3-SCR activity in the entire temperature range [14].

Fig. 5(B) shows the *in situ* DRIFTS results of NO_x adsorption over Nb_2O_5 and $CeNb_aZr_2O_x$ catalysts. After NO + O_2 adsorption for 1.0 h and N_2 purge for another 0.5 h, a couple of distinct bands assigned to bidentate nitrate (1583 and 1560 cm^{-1}) and bridging nitrate (1609, 1622, 1237 and 1217 cm^{-1}) were observed [34,38–40]. It was quite clear that the introduction of Nb decreased both the intensity and quantity of bands assigned to nitrate species, which might arise from the fact that the addition of Nb promoted the formation of more acid sites together with fewer alkali sites where the nitrate species adsorbed [33]. It was also reported that the adsorption of nitrate species on MnO_x–NbO_x–CeO_2 was weaker than that on MnO_x–CeO_2 as a result of Nb addition [37].

3.3.5. Reactivity of adsorbed NH_3 species

The *in situ* DRIFTS reaction between pre-adsorbed NH_3 and NO + O_2 at 200 °C was conducted to investigate the reactivity of adsorbed NH_3 species. As shown in Fig. 6(A), the surface of $CeZr_2O_x$ was mainly covered by ionic NH_4^+ (1414 and 1444 cm^{-1}) and coordinated NH_3 (3360, 3260, 1263 and 1160 cm^{-1}) after the catalyst was pre-adsorbed to NH_3. After the introduction of NO + O_2, the bands at 1160 cm^{-1} diminished in 5 min. However, the bands centered at 1444, 1414 and 1263 cm^{-1} were almost the same in 60 min, which might indicate that the adsorbed NH_3 species over $CeZr_2O_x$ were less active in the SCR reaction.

Compared to $CeZr_2O_x$, in Fig. 6(B), when NO + O_2 was introduced to $CeNb_{3.0}Zr_2O_x$ which was pre-exposed to NH_3, ionic NH_4^+ (1668 and 1434 cm^{-1}) and coordinated NH_3 (3360, 3260, 3155, 1603 and 1209 cm^{-1}) showed an apparent decrease in intensity due to the reaction between NO + O_2 and NH_3 species. After 3 min, all bands ascribed to NH_3 species were replaced by nitrate species. The results indicated that both ionic NH_4^+ and coordinated NH_3 on $CeNb_{3.0}Zr_2O_x$ were quite active in the SCR reaction. Therefore, it was safe to reach the conclusion that the introduction of Nb significantly improved the reaction activity of adsorbed NH_3 species on $CeNb_{3.0}Zr_2O_x$.

3.3.6. Reactivity of adsorbed NO_x species

The reactivity of adsorbed NO_x species in NH_3-SCR reaction on $CeZr_2O_x$ and $CeNb_{3.0}Zr_2O_x$ catalysts was also examined by the *in situ* DRIFTS of reaction between pre-adsorbed NO_x and NH_3 at 200 °C. For the $CeZr_2O_x$ catalyst (Fig. 7(A)), after NO + O_2 pre-adsorption and N_2 purging, the catalyst surface was covered with bidentate nitrate (1583 and 1560 cm^{-1}) along with bridging nitrate (1609, 1217 and 1237 cm^{-1}). When NH_3 was introduced, the intensity of the bands attributed to nitrate species did not show an obvious change. The adsorbed nitrate could not easily react with NH_3 species. The results indicated that the adsorbed nitrate species over $CeZr_2O_x$ catalyst were mostly inactive during the NH_3-SCR process.

As shown in Fig. 7(B), the surface of $CeNb_{3.0}Zr_2O_x$ catalyst was mainly covered by bridging nitrate centered at 1622 and 1217 cm^{-1} and bidentate species around 1583 cm^{-1} after exposed to NO + O_2. When NH_3 was introduced, the bands ascribed to bridging nitrate species were totally consumed in 3 min, however, the bidentate species did not decrease obviously which might indicate that the bridging nitrate rather than bidentate nitrate could react with NH_3. In addition, the bands corresponding to ionic NH_4^+ and coordinated NH_3 were appeared after 5 min. From the comparison between Fig. 7(A) and (B), it was believed that the adsorbed nitrate species on $CeNb_{3.0}Zr_2O_x$ were more reactive than those on $CeZr_2O_x$, which resulted in the enhanced NH_3-SCR activity.

It was believed that the redox ability and adsorption of NH_3 and NO_x of the catalysts played important roles in the NH_3-SCR reaction. In the present study, the $CeNb_{3.0}Zr_2O_x$ catalyst exhibited higher redox ability than the $CeZr_2O_x$, indicating that the $CeNb_{3.0}Zr_2O_x$

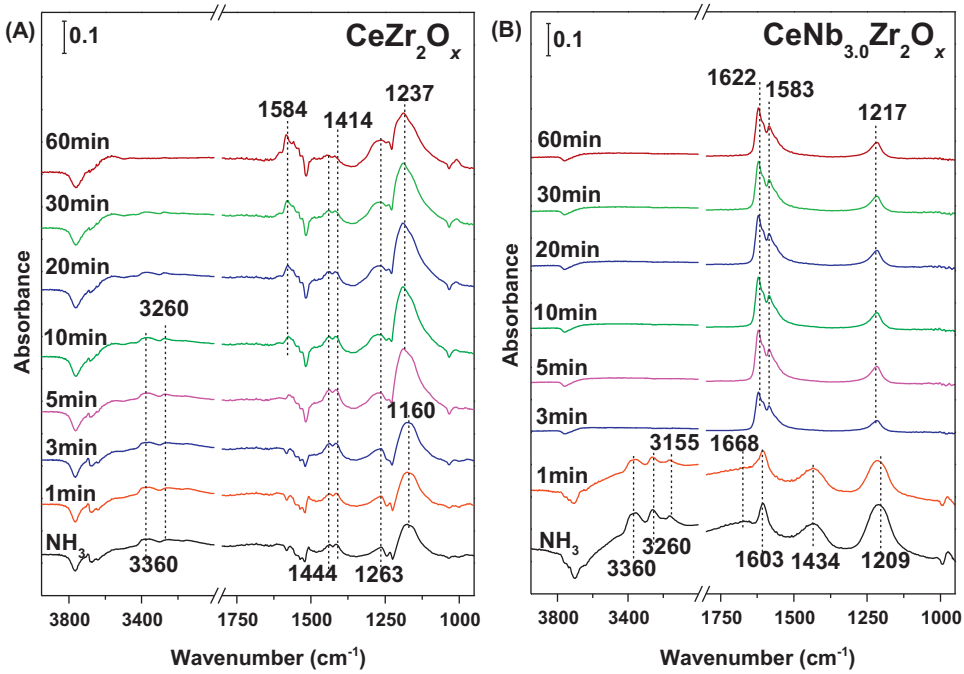

Fig. 6. *In situ* DRIFTS of NO + O_2 reacted with pre-adsorbed NH3 species at 200 °C on $CeZr_2O_x$ (A) and $CeNb_{3.0}Zr_2O_x$ (B) catalysts.

possessed high oxidation ability of NO to NO_2, which was beneficial for the so-called "fast SCR". On one hand, the addition of Nb promoted the adsorption and activation of NH_3, which were considered to be a key step in the NH_3-SCR process. On the other hand, the adsorption of nitrate species over $CeNb_{3.0}Zr_2O_x$ was weaker than that over $CeZr_2O_x$, due to the fact that the addition of Nb decreased the amount of basic sites where nitrate adsorbed. However, the reaction activity of adsorbed NH_3 and nitrate species over $CeNb_{3.0}Zr_2O_x$ was higher than that over $CeZr_2O_x$, and both of them could participate in the NH_3-SCR reaction according to the *in-situ* DRIFTS results. It was likely to conclude that the adsorbed NH_3 species could react with adsorbed nitrate to form N_2 and H_2O following the Langmuir–Hinshelwood (L–H) mechanism at 200 °C.

3.4. Promotional effect of Nb addition on the hydrothermal stability

3.4.1. Hydrothermal stability test over $CeNb_{3.0}Zr_2O_x$ and $CeZr_2O_x$ catalysts

The hydrothermal stability of NH_3-SCR catalysts is required in the long deNO_x for practical applications, as the diesel engine exhaust temperature can reach as high as 700 °C during the regeneration process of DPF system [41]. Accordingly, the $CeNb_{3.0}Zr_2O_x$

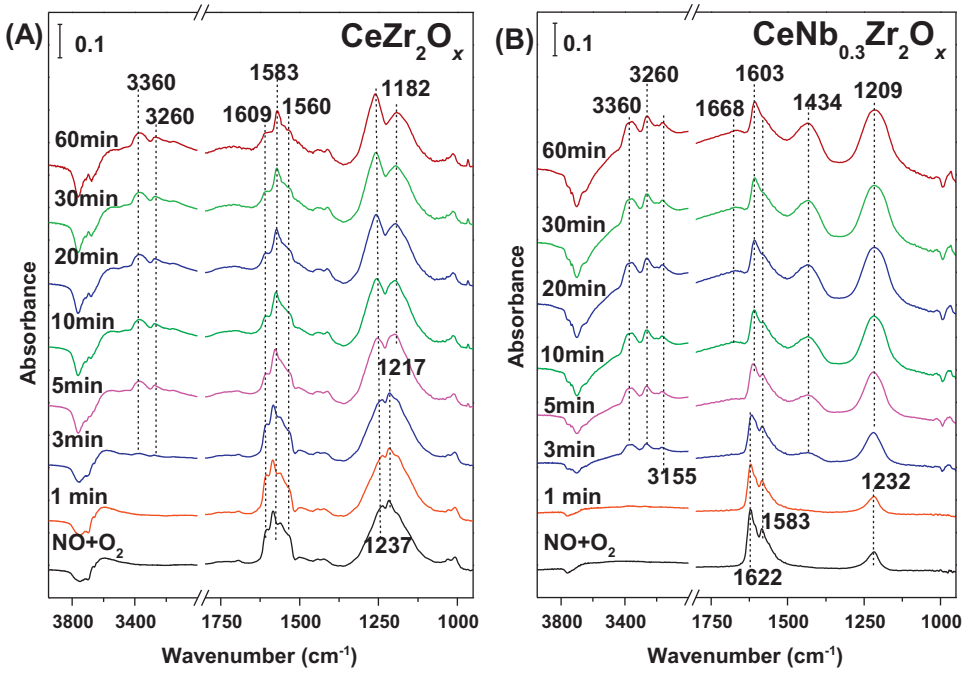

Fig. 7. *In situ* DRIFTS of NH_3 reacted with pre-adsorbed NO_x species at 200 °C on $CeZr_2O_x$ (A) and $CeNb_{3.0}Zr_2O_x$ (B) catalysts.

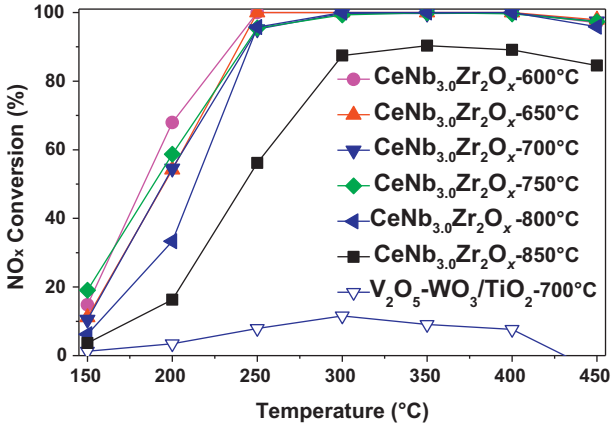

Fig. 8. NO_x conversion in NH_3-SCR reaction as a function of temperature over V_2O_5–WO_3/TiO_2 and $CeNb_{0.3}Zr_2O_x$ catalysts aged in air containing 10 vol.% H_2O at different temperatures for 8 h. Reaction conditions: [NO] = [NH_3] = 500 ppm, [O_2] = 5 vol.%, GHSV = 50,000 h^{-1}.

catalysts were hydrothermally aged at various temperatures for 8 h and the results are illustrated in Fig. 8. It was obvious that after hydrothermal treatment between 600 and 750 °C for 8 h, $CeNb_{3.0}Zr_2O_x$ catalysts showed similar SCR activity, over which more than 90% NO_x conversion was obtained in the temperature range of 250–450 °C. However, further improving the hydrothermal treatment temperature to 800 and 850 °C resulted in an obvious decrease of SCR activity, which might due to the sintering of active component. In addition, as shown in Fig. 9, $CeNb_{3.0}Zr_2O_x$ catalyst hydrothermally treated at 800 °C for 48 h still exhibited high NH_3-SCR activity, over which more than 80% NO_x conversion was obtained above 300 °C. For comparison purpose, the SCR activity of commercial V_2O_5–WO_3/TiO_2 catalyst treated in air containing 10 vol.% H_2O at 700 °C was also studied. The fresh V_2O_5–WO_3/TiO_2 catalyst exhibited high activity with more than 90% NO_x conversion from 250 to 450 °C (see Fig. S5). Nevertheless, the NO_x conversion reduced to less than 10% in the whole temperature range after hydrothermal aging at 700 °C for 8 h. Consequently, the $CeNb_{3.0}Zr_2O_x$ showed excellent hydrothermal stability compared to conventional V-based catalyst and was a promising candidate for the removal of NO_x from diesel engine exhaust. The $CeZr_2O_x$ catalysts were also hydrothermally aged at various temperatures to investigate the influence of Nb additive on the hydrothermal stability of Nb containing catalysts. As shown in Fig. S6, as the calcination temperature increased from 600 to 850 °C, the NO_x

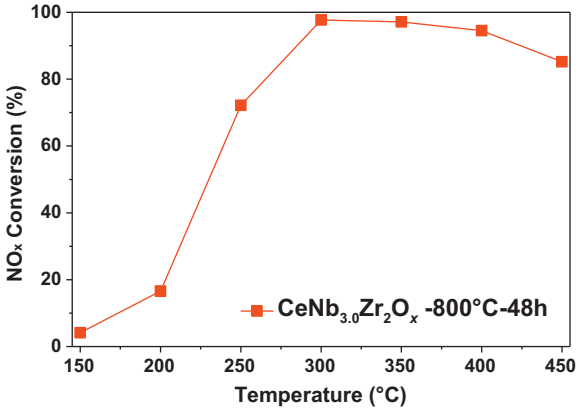

Fig. 9. NO_x conversion in NH_3-SCR reaction as a function of temperature over $CeNb_{3.0}Zr_2O_x$ catalysts aged in air containing 10 vol.% H_2O at 800 °C for 48 h. Reaction conditions: [NO] = [NH_3] = 500 ppm, [O_2] = 5 vol.%, GHSV = 50,000 h^{-1}.

Table 2
BET surface area, pore volume and H_2 consumption of $CeNb_{3.0}Zr_2O_x$ samples hydrothermally aged at various temperatures for 8 h

Catalysts	S_{BET}[a] (m^2/g)	Pore volume[b] (cm^3/g)	H_2 consumption (μmol H_2/g_{cat})
$CeNb_{3.0}Zr_2O_x$–600 °C	136.7	0.22	469.3
$CeNb_{3.0}Zr_2O_x$–650 °C	123.5	0.22	464.2
$CeNb_{3.0}Zr_2O_x$–700 °C	83.5	0.11	109.7
$CeNb_{3.0}Zr_2O_x$–750 °C	85.7	0.09	93.3
$CeNb_{3.0}Zr_2O_x$–800 °C	85.0	0.15	73.9
$CeNb_{3.0}Zr_2O_x$–850 °C	88.5	0.13	–

[a] BET surface area.[b]Total pore volume

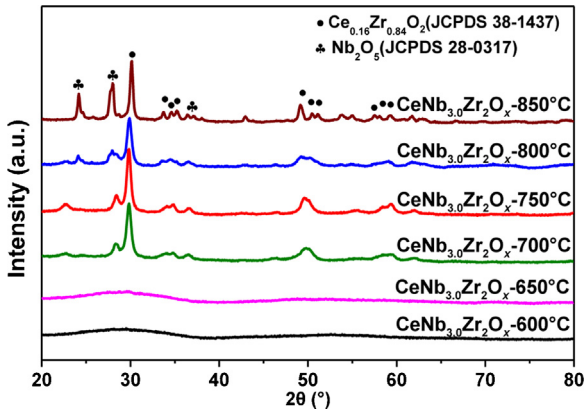

Fig. 10. Powder XRD results of $CeNb_{3.0}Zr_2O_x$ catalysts hydrothermally aged at different temperatures for 8 h.

conversion showed a monotonic decline in the entire temperature range. In combination with the results from Fig. 8 and S6, it was likely to conclude that the introduction of Nb to $CeZr_2O_x$ significantly improved the hydrothermal stability of $CeNb_{3.0}Zr_2O_x$. The reasons which were responsible for the high hydrothermal stability of $CeNb_{3.0}Zr_2O_x$ catalyst will be discussed later in this work.

3.4.2. N_2 physisorption

As shown in Fig. S7, the closure point of the hysteresis loops of the samples moved to higher P/P_0 with the increase of hydrothermal aging temperature, indicating that more abundant macropores were formed after hydrothermal aging. Besides, the surface area and pore volume of $CeNb_{3.0}Zr_2O_x$ catalysts hydrothermally treated at different temperatures for 8 h are illustrated in Table 2. It was obvious that increasing the temperature from 600 to 700 °C gave rise to a decline of surface area from 136.7 to 83.5 m^2/g. Nevertheless, the catalysts treated at 700–850 °C exhibited similar surface area about 85 m^2/g, which indicated that the reduce of surface area resulting from high temperature sintering had reached to the limit above 700 °C, and surface area might not be the main factor that was responsible for the differences of NO_x conversion.

3.4.3. XRD results

In addition, the crystal structure of $CeNb_{3.0}Zr_2O_x$ catalysts after hydrothermal aging was also investigated. As shown in Fig. 10, the $CeNb_{3.0}Zr_2O_x$ catalysts aged at 600 and 650 °C for 8 h showed similar XRD pattern, indicating that the $CeNb_{3.0}Zr_2O_x$ exhibited strong hydrothermal durability below 650 °C. Further increasing the aging temperature to 700 °C above resulted in the formation of Nb_2O_5 and $Ce_{0.16}Zr_{0.84}O_2$ solid solution due to the incorporation of Zr^{4+} with a smaller radius into the lattice of CeO_2 [42]. It was interesting that even after the treatment at 700, 750 and 800 °C, $CeNb_{3.0}Zr_2O_x$ catalyst still remained more than 90% NO_x conver-

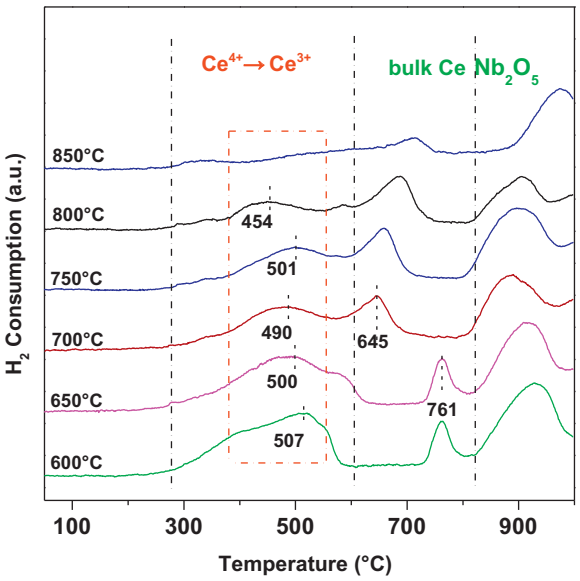

Fig. 11. H_2-TPR profiles of $CeNb_{3.0}Zr_2O_x$ catalysts hydrothermally aged at various temperatures.

sion above 250 °C, which might suggest that the $Ce_{0.16}Zr_{0.84}O_2$ solid solution was also active in NH_3-SCR reaction. Furthermore, large amount of $Ce_{0.16}Zr_{0.84}O_2$ solid solution still existed in the $CeNb_{3.0}Zr_2O_x$ catalyst hydrothermally treated at 850 °C. However, $CeNb_{3.0}Zr_2O_x$–850 °C catalyst exhibited poor SCR activity, indicating that some other factors were also essential for the activity.

3.4.4. H_2-TPR

The H_2-TPR results of hydrothermally aged $CeNb_{3.0}Zr_2O_x$ catalysts are illustrated in Fig. 11. For all the catalysts, the reduction peaks less than 600 °C belonged to the reduction of surface Ce^{4+}, and the peaks centered at high temperatures were ascribed to the reduction of bulk CeO_2 and Nb_2O_5. In addition, the H_2 consumption for the reduction of surface Ce^{4+} to Ce^{3+} was listed in Table 2, and it was clear that increasing the hydrothermal aging temperature from 600 to 800 °C resulted in a decrease of the H_2 consumption from 469.3 to 73.9 μmol H_2/g_{cat}. The catalysts hydrothermally aged at less than 750 °C showed similar reduction peaks centered at about 500 °C. It was likely that the similar reduction temperature was responsible for the similar NH_3-SCR activity. $CeNb_{3.0}Zr_2O_x$–800 °C sample showed a relative low reduction temperature around 454 °C, indicating that it should exhibit high activity. However, the lack of enough reducible surface Ce^{4+} lowered SCR conversion. For $CeNb_{3.0}Zr_2O_x$–850 °C sample, no obvious peak ascribed to Ce^{4+} reduction was observed, which was in highly agreement with the poor NO_x conversion. It was worth mentioning that the peaks attributed to bulk Ce showed an abrupt shift from 761 to 645 °C, as the hydrothermal treatment temperature increased from 650 to 700 °C. This may be connected with the structural change, which was proved to be true by the XRD results in Fig. 6, as the hydrothermal treatment at 700 °C led to the formation of $Ce_{0.16}Zr_{0.84}O_2$ solid solution.

3.4.5. NH_3 and NO_x adsorption ability

In order to further investigate the influence of hydrothermal treatment on the adsorption ability of reaction species, the *in situ* DRIFTS of NH_3 and NO_x adsorption at 200 °C were conducted and the results are shown in Fig. 12(A) and (B), respectively. As shown in Fig. 12(A), no obvious band ascribed to adsorbed NH_3 species was observed on $CeNb_{3.0}Zr_2O_x$ catalyst hydrothermally aged at 850 °C. However, $CeNb_{3.0}Zr_2O_x$–800 °C sample still possessed large amount of adsorbed NH_3 species. The total amount of adsorbed NH_3 species over $CeNb_{3.0}Zr_2O_x$–650 °C, $CeNb_{3.0}Zr_2O_x$–700 °C and $CeNb_{3.0}Zr_2O_x$–750 °C was similar. As mentioned before, acid sites played a significant role in the adsorption and activation of NH_3 during the SCR process. Therefore, in combination with the H_2-TPR results of hydrothermal aged $CeNb_{3.0}Zr_2O_x$ samples in Fig. 11, it was reasonable that the $CeNb_{3.0}Zr_2O_x$ catalysts hydrothermally aged between 650 and 750 °C showed similar SCR activity. In addition, the amount of adsorbed NO_3^- presented a minor decline with increasing aging temperature indicating that the basic sites over $CeNb_{3.0}Zr_2O_x$ were diminished after hydrothermal aging.

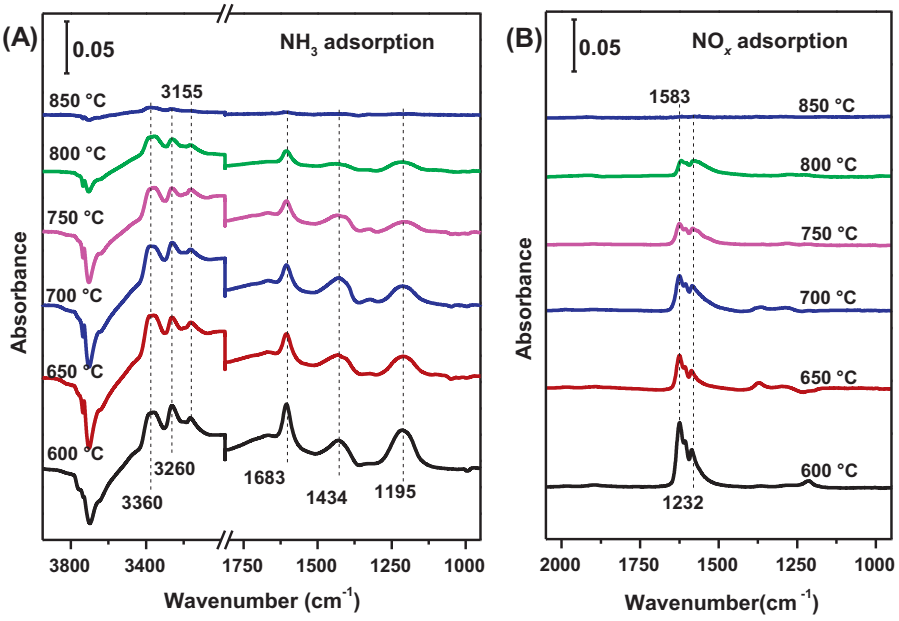

Fig. 12. *In situ* DRIFTS of 500 ppm NH_3 adsorption (A) and 500 ppm NO + 5 vol.% O_2 adsorption (B) with 300 mL/min flow rate at 200 °C on $CeNb_{3.0}Zr_2O_x$ catalysts hydrothermally treated at various temperatures.

4. Conclusions

A novel Nb doped $CeZr_2O_x$ catalyst prepared by a homogeneous precipitation was used in the NH_3-SCR reaction. $CeNb_{3.0}Zr_2O_x$ catalyst with the Nb/Ce molar ratio of 3.0:1 showed excellent SCR activity along with high N_2 selectivity, SO_2/H_2O resistance and remarkable hydrothermal stability. The characterization results demonstrated that the $CeNb_{3.0}Zr_2O_x$ catalyst, a promising NH_3-SCR catalyst, possessed large surface area, strong redox ability and high reactive nitrate together with NH_3 species, all of which were responsible for the remarkable SCR performance. Furthermore, the $CeNb_{3.0}Zr_2O_x$ catalyst still remained high redox ability together with affluent acid sites after hydrothermal aging below 800 °C, and was a promising candidate for the elimination of NO_x from diesel engine exhaust.

Acknowledgements

This work was supported by the National Natural Science Foundation of China (51221892) and the Ministry of Science and Technology, China (2013AA065301).

Appendix A. Supplementary data

Supplementary data associated with this article can be found, in the online version, at http://dx.doi.org/10.1016/j.apcatb.2015.06.055

References

[1] H. Bosch, F. Janssen, Formation and control of nitrogen oxides, Catal. Today 2 (1988) 369–379.
[2] G. Busca, L. Lietti, G. Ramis, F. Berti, Chemical and mechanistic aspects of the selective catalytic reduction of NO_x by ammonia over oxide catalysts: a review, Appl. Catal. B: Environ. 18 (1998) 1–36.
[3] V.I. Pavulescu, P. Grange, B. Delmon, Catalytic removal of NO, Catal. Today 46 (1998) 233–316.
[4] F.D. Liu, H. He, Y. Ding, C.B. Zhang, Effect of manganese substitution on the structure and activity of iron titanate catalyst for the selective catalytic reduction of NO with NH_3, Appl. Catal. B: Environ. 93 (2009) 194–204.
[5] J.P. Dunn, P.R. Koppula, H.G. Stenger, I.E. Wachs, Oxidation of sulfur dioxide to sulfur trioxide over supported vanadia catalysts, Appl. Catal. B: Environ. 19 (1998) 103–117.
[6] J. Kašpar, P. Fornasiero, M. Graziani, Use of CeO_2-based oxides in the three-way catalysis, Catal. Today 50 (1999) 285–298.
[7] H.W. Jen, G.W. Graham, W. Chun, R.W. McCabe, J.P. Cuif, S.E. Deutsch, O. Touret, Characterization of model automotive exhaust catalysts: Pd on ceria and ceria–zirconia supports, Catal. Today 50 (1999) 309–328.
[8] M. Haneda, T. Morita, Y. Nagao, Y. Kintaichi, H. Hamada, CeO_2–ZrO_2 binary oxides for NO_x removal by sorption, Phys. Chem. Chem. Phys. 3 (2001) 4696–4700.
[9] Y. Li, H. Cheng, D. Li, Y. Qin, Y. Xie, S. Wang, WO_3/CeO_2–ZrO_2, a promising catalyst for selective catalytic reduction (SCR) of NO_x with NH_3 in diesel exhaust, Chem. Commun. 12 (2008) 1470–1472.
[10] S. Gao, X. Chen, H. Wang, J. Mo, Z. Wu, Y. Liu, X. Weng, Ceria supported on sulfated zirconia as a superacid catalyst for selective catalytic reduction of NO with NH_3, J. Colliod Interface Sci. 394 (2013) 515–521.
[11] Z.C. Si, D. Weng, X.D. Wu, R. Ran, Z.R. Ma, NH_3-SCR activity, hydrothermal stability sulfur resistance and regeneration of $Ce_{0.75}Zr_{0.25}O_2$–PO_4^{3-} catalyst, Catal. Commun. 17 (2012) 146–149.
[12] R.H. Gao, D.S. Zhang, P. Maitarad, L.Y. Shi, T. Rungrotmongkol, H.R. Li, J.P. Zhang, W.G. Cao, Morphology-dependent properties of MnO_x/ZrO_2–CeO_2 nanostructures for the selective catalytic reduction of NO with NH_3, J. Phys. Chem. C 117 (2013) 10502–10511.
[13] P. Maitarad, D.S. Zhang, R.H. Gao, L.Y. Shi, H.R. Li, L. Huang, T. Rungrotmongkol, J.P. Zhang, Combination of experimental and theoretical investigations of $MnO_x/Ce_{0.9}Zr_{0.1}O_2$ nanorods for selective catalytic reduction of NO with ammonia, J. Phys. Chem. C 117 (2013) 9999–10006.
[14] Z. Lian, F. Liu, H. He, X. Shi, J. Mo, Z. Wu, Manganese–niobium mixed oxide catalyst for the selective catalytic reduction of NO_x with NH_3 at low temperatures, Chem. Eng. J. 250 (2014) 390–398.
[15] M. Casapu, O. Krocher, M. Mehring, M. Nachtegaal, C. Borca, M. Harfouche, D. Grolimund, Characterization of Nb-containing MnO_x–CeO_2 catalyst for low-temperature selective catalytic reduction of NO with NH_3, J. Phys. Chem. C 114 (2010) 9791–9801.
[16] R. Qu, X. Gao, K. Cen, J. Li, Relationship between structure and performance of a novel cerium–niobium binary oxide catalyst for selective catalytic reduction of NO with NH_3, Appl. Catal. B: Environ. 142 (2013) 290–297.
[17] K.S.W. Sing, D.H. Everett, R.A.W. Haul, L. Moscou, R.A. Pierotti, J. Rouquerol, T. Siemieniewska, Reporting physisorption data for gas solid systems with special reference to the determination of surface-area and porosity (recommendations 1984), Pure Appl. Chem. 57 (1985) 603–619.
[18] S. Gao, P. Wang, X. Chen, H. Wang, Z. Wu, Y. Liu, X. Weng, Enhanced alkali resistance of CeO_2/SO_4^{2-}–ZrO_2 catalyst in selective catalytic reduction of NO_x by ammonia, Catal. Commun. 43 (2014) 223–226.
[19] P. Li, Y. Xin, Q. Li, Z.P. Wang, Z.L. Zhang, L.R. Zheng, Ce–Ti amorphous oxides for selective catalytic reduction of NO with NH_3: confirmation of Ce–O–Ti active sites, Environ. Sci. Technol. 46 (2012) 9600–9605.
[20] Z. Liu, J. Zhu, J. Li, L. Ma, S.I. Woo, Novel Mn–Ce–Ti mixed-oxide catalyst for the selective catalytic reduction of NO_x with NH_3, ACS Appl. Mater. Interfaces 6 (2014) 14500–14508.
[21] X. Li, Y. Li, Selective catalytic reduction of NO with NH_3 over $CeMoO_x$ catalyst, Catal. Lett. 144 (2013) 165–171.
[22] Y. Peng, J. Li, L. Chen, J. Chen, J. Han, H. Zhang, W. Han, Alkali metal poisoning of a CeO_2–WO_3 catalyst used in the selective catalytic reduction of NO_x with NH_3: an experimental and theoretical study, Environ. Sci. Technol. 46 (2012) 2864–2869.
[23] Z. Lian, F. Liu, H. He, Effect of preparation methods on the activity of VO_x/CeO_2 catalysts for the selective catalytic reduction of NO_x with NH_3, Catal. Sci. Technol. 5 (2014) 389–396.
[24] I.E. Wachs, L.E. Briand, J.-M. Jehng, L. Burcham, X. Gao, Molecular structure and reactivity of the group V metal oxides, Catal. Today 57 (2000) 323–330.
[25] H. Xu, Y. Wang, Y. Cao, Z. Fang, T. Lin, M. Gong, Y. Chen, Catalytic performance of acidic zirconium-based composite oxides monolithic catalyst on selective catalytic reduction of NO_x with NH_3, Chem. Eng. J. 240 (2014) 62–73.
[26] S. Cai, D. Zhang, L. Zhang, L. Huang, H. Li, R. Gao, L. Shi, J. Zhang, Comparative study of 3D ordered macroporous $Ce_{0.75}Zr_{0.2}M_{0.05}O_{2-\delta}$((M = Fe, Cu, Mn, Co) for selective catalytic reduction of NO with NH_3, Catal. Sci. Technol. 4 (2014) 93–101.
[27] J. Yu, Z.C. Si, L. Chen, X.D. Wu, D. Weng, Selective catalytic reduction of NO_x by ammonia over phosphate-containing $Ce_{0.75}Zr_{0.25}O_2$ solids, Appl. Catal. B: Environ. 163 (2015) 223–232.
[28] S.Y. Christou, M.C. Alvarez-Galvan, J.L.G. Fierro, A.M. Efstathiou, Suppression of the oxygen storage and release kinetics in $Ce_{0.5}Zr_{0.5}O_2$ induced by P, Ca and Zn chemical poisoning, Appl. Catal. B: Environ. 106 (2011) 103–113.
[29] B.Q. Jiang, Z.G. Li, S.C. Lee, Mechanism study of the promotional effect of O_2 on low-temperature SCR reaction on Fe–Mn/TiO_2 by DRIFT, Chem. Eng. J. 225 (2013) 52–58.
[30] L. Chen, J. Li, M. Ge, DRIFT study on cerium–tungsten/titania catalyst for selective catalytic reduction of NO_x with NH_3, Environ. Sci. Technol. 44 (2010) 9590–9596.
[31] X.L. Li, Y.H. Li, Molybdenum modified $CeAlO_x$ catalyst for the selective catalytic reduction of NO with NH_3, J. Mol. Catal. A: Chem. 386 (2014) 69–77.
[32] W.P. Shan, F.D. Liu, H. He, X.Y. Shi, C.B. Zhang, A superior Ce–W–Ti mixed oxide catalyst for the selective catalytic reduction of NO_x with NH_3, Appl. Catal. B: Environ. 115 (2012) 100–106.
[33] Z.M. Liu, S.X. Zhang, J.H. Li, L.L. Ma, Promoting effect of MoO_3 on the NO_x reduction by NH_3 over CeO_2/TiO_2 catalyst studied with *in situ* DRIFTS, Appl. Catal. B: Environ. 144 (2014) 90–95.
[34] Z.B. Wu, B.Q. Jiang, Y. Liu, H.Q. Wang, R.B. Jin, DRIFT study of manganese/titania-based catalysts for low-temperature selective catalytic reduction of NO with NH_3, Environ. Sci. Technol. 41 (2007) 5812–5817.
[35] N.Y. Topsoe, Mechanism of the selective catalytic reduction of nitric oxide by ammonia elucidated by *in situ* on-line Fourier transform infrared spectroscopy, Science 265 (1994) 1217–1219.
[36] L. Chen, J.H. Li, M.F. Ge, L. Ma, H.Z. Chang, Mechanism of selective catalytic reduction of NO_x with NH_3 over CeO_2–WO_3 catalysts, Chin. J. Catal. 32 (2011) 836–841.
[37] M. Casapu, O. Kroecher, M. Mehring, M. Nachtegaal, C. Borca, M. Harfouche, D. Grolimund, Characterization of Nb-containing MnO_x–CeO_2 catalyst for low-temperature selective catalytic reduction of NO with NH_3, J. Phys. Chem. C 114 (2010) 9791–9801.
[38] F.D. Liu, K. Asakura, H. He, Y.C. Liu, W.P. Shan, X.Y. Shi, C.B. Zhang, Influence of calcination temperature on iron titanate catalyst for the selective catalytic reduction of NO_x with NH_3, Catal. Today 164 (2011) 520–527.
[39] F.D. Liu, W.P. Shan, Z.H. Lian, L.J. Xie, W.W. Yang, H. He, Novel $MnWO_x$ catalyst with remarkable performance for low temperature NH_3-SCR of NO_x, Catal. Sci. Technol. 3 (2013) 2699–2707.
[40] B. Tsyntsarski, V. Avreyska, H. Kolev, T. Marinova, D. Klissurski, K. Hadjiivanov, FT-IR study of the nature and reactivity of surface NO_x compounds formed after NO adsorption and NO + O_2 coadsorption on zirconia- and sulfated zirconia-supported cobalt, J. Mol. Catal. A: Chem. 193 (2003) 139–149.
[41] X.Q. Wang, A.J. Shi, Y.F. Duan, J. Wang, M.Q. Shen, Catalytic performance and hydrothermal durability of CeO_2–V_2O_5–ZrO_2/WO_3–TiO_2 based NH_3-SCR catalysts, Catal. Sci. Technol. 2 (2012) 1386–1395.
[42] J. Liu, Z. Zhao, C. Xu, A. Duan, L. Wang, S. Zhang, Synthesis of nanopowder Ce–Zr–Pr oxide solid solutions and their catalytic performances for soot combustion, Catal. Commun. 8 (2007) 220–224.